FINAL REPORT

INTEGRATING P-WAVE AND S-WAVE SEISMIC DATA TO IMPROVE CHARACTERIZATION OF OIL RESERVOIRS

by

Innocent J. Aluka

Prepared for U.S. Department of Energy
Under Grant No. DE-FG26-00NT40832

Department of Physics/Physical Science
Prairie View A&M University
P.O. Box 2516
Prairie View,
TX 77446
December 2004

Report Title: **Integrating P-Wave and S-Wave Seismic Data to Improve Characterization of Oil Reservoirs**

Type of Report: **Final**

Reporting Period Start Date: **September 1, 2000**

Reporting Period End Date: **August 31, 2004**

Principal Author: **Innocent J. Aluka**

Date of Report: **December 7, 2004**

Grant Number: **DE-FG26-00NT40832**

Institution: **Prairie View A&M University**

Subcontractor: **Bureau of Economic Geology, Austin, Texas 78713**

Industrial Collaborator: **Seismic Micro-Technology, Inc; Houston**

Address: **P.O. Box 2516, Prairie View, TX 77446**

DISCLAIMER

ABSTRACT

The data used in this study were acquired by nine-component (9C) vertical seismic profile (VSP), using three orthogonal vector sources. The 9C vertical seismic profile is capable of generating P-wave mode and the fundamental S-wave mode (SH-SH and SV-SV) directly at the source station and permits the basic components of elastic wavefield (P, SH-SH and SV-SV) to be separated from one another for the purposes of imaging. Analysis and interpretations of data from the study area show that incident full-elastic seismic wavefield is capable of reflecting four different wave modes, P, SH , SV and C which can be utilized to fully understand the architecture and heterogeneities of geologic sequences. The conventional seismic stratigraphy utilizes only reflected P-wave modes. The notation SH mode is the same as SH-SH; SV mode means SV-SV and C mode which is a converted shear wave is a special SV mode and is the same as P-SV.

These four wave modes image unique geologic stratigraphy and facies and at the same time reflect independent stratal surfaces because of the unique orientation of their particle-displacement vectors. As a result of the distinct orientation of individual mode's particle-displacement vector, one mode may react to a critical subsurface sequence more than the other. It was also observed that P-wave and S-wave do not always reflect from the same stratal boundaries. At inline coordinate 2100 and crossline coordinates of 10,380, 10430, 10480 and 10,520 the P-wave stratigraphy shows coherency at time slice 796 m/s and C-wave stratigraphy shows coherency at time slice 1964 m/s at the same inline coordinate and crossline coordinates of 10,400 to 10470. At inline cordinate 2800 and crossline coordinate 10,650, P-wave stratigraphy shows coherency at time slice 792 m/s and C-wave stratigraphy shows coherency at time slice 1968 m/s. The utilization of full-elastic seismic wavefield needs to be maximized in oil and gas explorations in order to optimize the search for hydrocarbons.

TABLE OF CONTENTS

FIGURES

Figure 7. P-wave image search target.

Figure 8. Depth-equivalent C-wave target.

Figure 9. Comparison of P-wave and C-wave image targets.

Figure 10. Contrast between P reflectivity $R_{i,p}$ and S reflectivity $R_{i,s}$ for vertical incidence on a stratal surface.

INTRODUCTION

The internal complexities and heterogeneities within the oil reservoir can be characterized with seismic stratigraphy. Traditionally, most oil reservoir characterization are done with only compressional P-wave seismic data. The full science of reservoir characterization can be achieved by incorporating the principles and applications of vector-wave field seismic data in which geologic systems are interpreted using both P-wave and shear (S) wave images of subsurface stratigraphy. This is so, because, sometimes spatially coincident P and S seismic profiles do not show the same reflection sequences or the same lateral variations in seismic facies character.

EXECUTIVE SUMMARY

The basic principle of seismic stratigraphy is that a seismic reflection event images a surafce of geologic sequence. The imaging of geologic sequence is accomplished by introducing an incident full-elastic seismic wavefield into the subsurface geologic sequences.
The incident full-elastic seismic wavefield reflected four different wave modes, P, fast-S (SH) , slow-S (SV) and C. These four wave modes reflect independent stratal surfaces and image different geologic architecture and facies. These wave modes were generated by nine-component vertical seismic profile.

The 3-D, 9-component data were recorded using midpoint imaging concepts that are standard practice in the oil and gas industry. Three orthogonal vibrators used to generate 9C (9-component) VSP (vertical seismic profile) are vertical vibrator, inline horizontal vibrator and crossline horizontal vibrator. The geometry of the three orthogonal vibrators created stacking bins measuring 110 ft x 82.5 ft across the image space, with a stacking fold of 20 to 24 in the full-fold area of each data acquisition grid. The recording template that moved across the image space consisted of six parallel receiver lines, each spanning 96 receiver stations. Three-component geophones were deployed at each receiver station of this 3-D grid. Each receiver string deployed at a receiver station contained three 3-C geophones, and all three geophones were positioned in an area spanning 3 to 5 feet to form a point array. The geophones were planted carefully to position one horizontal element in the inline direction (the direction that the receiver line was oriented) and the second horizontal element in the crossline direction.

Large (52,000 lb) vibrators were used to generate the 9-component data. Three distinct sets of vibrator units occupied each of the source stations. Vertical vibrators comprised one of these source arrays. These vertical vibrators generated a wavefield that was dominated by P-waves, and that wavefield was recorded by the rectangular grid of 3-component sensors in the recording template that was centered on the source station. S-wave dominated wavefields were generated by horizontal vibrators. One set of horizontal vibrators applied a shearing motion in the inline direction at each source station, and a second set of horizontal vibrators applied a shearing motion in the crossline direction. The wavefields produced by these two distinct polarized S-wave sources were recorded as individual records by the 6-line template of 3-C receivers centered on the active source station.

Data analysis shows that P-wave and S-wave do not always reflect from the same stratal boundaries. At inline coordinate 2100 and crossline coordinates of 10,380, 10430, 10480 and 10,520 the P-wave stratigraphy shows coherency at time slice 796 m/s and C-wave stratigraphy shows coherency at time slice 1964 m/s at the same inline coordinate and crossline coordinates of 10,400 to 10470. At inline cordinate 2800 and crossline coordinate 10,650, P-wave stratigraphy shows coherency at time slice 792 ms and C-wave stratigraphy shows coherency at time slice 1968 ms.

The P and C wave are capable of imaging different stratal surfaces because P and C modes have different reflectivities at impedance boundaries. It was observed that it is possible for either P or C mode to have a zero , or near-zero reflectivity at a given stratal geologic surface while the other mode has a large reflevtivity.

EXPERIMENTAL

The analysis was carried out on PCs, utilizing the software provided by the Seismic Micro-Technology, Inc; (SMT).

The main service software package provided by Seismic Micro-Technology, Inc; (SMT) include 2d/3dPAK data interpretation, 2d/3d Seismic Interpretation, The Kingdom Suite SynPAK, The Kingdom Suite VuPAK, The Kingdom Suite TracePAK, The Kingdom Suite ModPAK , and the EarthPAK.

RESULTS AND DISCUSSION

Conventional seismic stratigraphy is one of the major traditional tools used to detect the internal complexities and heterogeneities within oil reservoirs. But the concepts and principles of conventional seismic stratigraphy are based only on P-wave seismic data, with little or no applications of S-wave seismic data to reservoir characterization. The complete understanding of reservoir characterization can be achieved only by expanding the principles and concepts of conventional seismic stratigraphy to a new approach described as vector-wavefield seismic data in which geologic systems are interpreted using both P-wave and shear (S) wave (both fast-S, and slow-S data) images of the subsurface sequences. This is so, because, sometimes spatially coincident P and S seismic profiles do not show the same reflection sequences or the same lateral variations in seismic facies character. This observation leads to the conclusion that in complex geologic systems, the sedimentary record must be described by one set of P-wave seismic sequences (and facies) and also by a second, distinct set of S-wave seismic sequences (and facies). Figure 1 shows full-elastic, multicomponent seismic wavefield in a homogeneous earth consisting of a compressional mode P and two shear modes, SV and SH. The propagation procedures of these modes differ as indicated in figure 1. Note that each mode travels through the earth in a different direction along its propagation path.

Laboratory studies of P-wave velocity (Vp) and S-wave velocity (Vs) in cores have shown that the ratio Vp/Vs has a distinct value for different types of rocks. Also, these Vp/Vs ratios are consistent over a wide range of porosities and confining pressures, whereas, each velocity (Vp or Vs) varies when either porosity or confining pressure changes. Thus the combination of P and S seismic data provides a capability to identify subsurface distributions of rock types through Vp/Vs ratios that is not available from P-wave seismic data alone. Particularly important is the phenomenon that S-wave split into fast-S and slow-S components when they encounter strata that are highly anisotropic. This petrophysical sensitivity has been utilized to detect and map fractured rocks with surface-recorded S-wave reflection data. P-waves exhibit little sensitivity to anisotropic rock properties, compared to the sensitivity of S-waves. Thus, 9-component seismic data allow seismic stratigraphy concepts to be expanded into anisotropic rocks where conventional P-wave-based seismic stratigraphy does not apply, or applies in a limited, and weak fashion.

The 3-D, 9-component data used in the study were recorded using midpoint imaging concepts that are standard practice in the oil and gas industry. Three orthogonal vibrators used to generate 9C (9-component) VSP (vertical seismic profile) are vertical vibrator, inline horizontal vibrator and crossline horizontal vibrator (figure 2).
The geometry of the three orthogonal vibrators created stacking bins measuring 110 ft x 82.5 ft across the image space, with a stacking fold of 20 to 24 in the full-fold area of each data acquisition grid. The recording template that moved across the image space consisted of six parallel receiver lines, each spanning 96 receiver stations. Three-component geophones were deployed at each receiver station of this 3-D grid. Each receiver string deployed at a receiver station contained three 3-C geophones, and all three geophones were positioned in an area spanning 3 to 5 feet to form a point array. The geophones were planted carefully to position one horizontal element in the inline direction (the direction that the receiver line was oriented) and the second horizontal element in the crossline direction.

Large (52,000 lb) vibrators were used to generate the 9-component data. Three distinct sets of vibrator units occupied each of the source stations. Vertical vibrators comprised one of these source arrays. These vertical vibrators generated a wavefield that was dominated by P-waves, and that wavefield was recorded by the rectangular grid of 3-component sensors in the recording template that was centered on the source station. S-wave dominated wavefields were generated by horizontal vibrators. One set of horizontal vibrators applied a shearing motion in the inline direction at each source station, and a second set of horizontal vibrators applied a shearing motion in the crossline direction. The wavefields produced by these two distinct polarized S-wave sources were recorded as individual records by the 6-line template of 3-C receivers centered on the active source station. Figure 3 shows the fundamental geometry necessary for 9C vertical seismic profile data acquisition. The source vector P indicates the force applied by the vertical vibrator. S_{IL} is the force vector applied by the horizontal vibrator, and S_{XL} is the force vector produced by the crossline vibrator. In this VSP data acquisition, inline is the direction from the source satation to the vertical receiver station, which is the orientation direction of the vertical plane ABCD. The crossline is the direction perpendicular to the inline, which is the direction normal to the plane ABCD.

Analysis of data shows that P and C waves often image different stratal surfaces.The propagation of incident full-elastic seismic wavefield generates four different wave modes, P-wave, SH-wave (horizontal shear wave), SV-wave (vertical shear wave) and C-wave (converted shear wave) as shown in figure 4. These four wave modes reflect

independent stratal surfaces. SH, SV, and C are three independent shear wave seismic modes. An upgoing SH mode can be produced by only a downgoing SH mode. The upgoing and downgoing modes are called SH-SH (SH down and SH up). SV is also called SV-SV, meaning SV down and SV up. C is a converted shear wave, meaning it is a special SV mode created by a downgoing P-wave. This is called P-SV, meaning P down and SV up.

Futher imaging differences between P and S-wave modes are illustrated by elastic wavefield stratigraphy (figures 5 through 10).
Coherency numerically measures lateral similarity of reflection waveforms in a defined data window. If the wavelet reflecting from an extensive interface has the same waveshape across the image space, the lateral coherency is high. On the other hand, if that interface is cut by a channel or incisement, for instance, the reflecting wavelet changes its waveshape at the edges of the channel. In such a case, lateral coherency is low across those narrow parts of the image space where the channel edges are. In a map of coherency, channels and incisements are shown as trends of low lateral wavelet coherency. At inline cordinate 2800 and crossline coordinate 10,650, both P and C modes show similar but not identical cross section of the incisement at each time-slice coordinate (figure 5). The white line across each seismic section indicates the position of the time slice in each data volume that is used in the image displays; the vertical black bars mark the edge of the incised feature. In figure 6 the P-wave data no longer have a distinct character, while C-wave data has a prominent characteristic. In figure 7, P-wave shows a complex system of overlapping, meandering channels but in figure 8, C-wave shows only one channel. Figure 9 compares both the P- wave and C-wave images.

Basic physics of P-wave and S-wave indicates different reflection behaviors and further shows that P-wave and S-wave do not produce identical images of stratal surfaces This is expressed mathematically as shown below:

REFLECTIVITY PARAMETERS

Layer (i) $(P_i,\ V_{p,i},\ V_{s,i}+1)$

Layer (i +1) $(P_{i+1},\ V_{p,i+1},\ V_{s,i+1})$

P AND S REFLECTION COEFFICIENTS

$$R_{i,s} = \frac{(PV_s)_{i+1} - (PV_s)_i}{(PV_s)_{i+1} + (PV_s)_i} \qquad R_{i,p} = \frac{(PV_p)_{i+1} - (PV_p)_i}{(PV_p)_{i+1} + (PV_p)_{i+1}}$$

$$R_{i,s} = \frac{Bi\,(1 - R_{i,p}) - (1 + R_{i,p})}{B_i(1 - R_{i,p}) + (1 + R_{i,p})} \qquad B_i = \frac{(V_p/V_s)_i + 1}{(V_p/V_s)_i}$$

These mathematical forms can be graphically expressed to relate P-wave reflectivity ($R_{i,p}$) to S-wave reflectivity ($R_{i,s}$) (figure 10). B_i is the horizontal axis. V_p is the P-wave velocity, V_s, the S-wave velocity, i is the upper geologic sequence, while i +1 is the underlying geologic sequence. The P-wave reflection coefficient ($R_{i,p}$) is the constant for each curve and the value is expressed on each curve. The curves show that if the P-wave reflection coefficient ($R_{i,p}$) is zero at any given geologic interface, the S-wave reflection coefficient can be zero, negative or positive, depending on the value of B_i. On the other hand, if the reflection coefficient of S-wave is zero at any given geologic boundary, the P-wave reflection coefficient may be zero, negative or positive, depending on the value of B_i.

This implies that full science of reservoir characterization can be achieved by incorporating the principles and applications of vector-wave field seismic data in which geologic systems are interpreted using both P-wave and shear (S) wave images of subsurface stratigraphy.

CONCLUSION

Since conventional seismic stratigraphy is limited when characterizing oil resevoirs because its concepts and principles have been developed and demonstrated using only P-wave seismic data, and at the same time have been verified using only P-wave technology; the complete science of reservoir characterization can be realized only by expanding its principles and applications to vector-wavefield seismic data in which geologic systems are interpreted using both P-wave and S-wave images of geologic sequences. This statement is based on the results of this study which showed that in some instances, spatially coincident P and S seismic profiles do not exhibit the same reflection sequences or the same lateral variations in seismic facies character. It is further concluded that in a complex geologic environment, it is necessary that sedimentary record be described by one set of P-wave seismic sequences(and facies) and also by a second, distinct set of S-wave seismic sequences (and facies). A full comprehension of geologic environment (reservoir architecture and heterogeneities) cannot be made until both P and S wave images are unified in seismic stratigraphy interpretations. The application of both P and S wave images to oil reservoir characterization is the current trend in most oil and gas companies and will sooner or later overtake the conventional seismic stratigraphy of only the P-wave imaging.

REFERENCES

1. **Hardage, B.A., 1996, Combining P-wave and S-wave seismic data to improve prospect evaluation: Report of Investigation No. 237, Bureau of Economic Geology, The University of Texas at Austin, 47 p.**

2. **McCormack, M.D., Sharp, W.W., and Dunbar, J.A., 1984, A case study of stratigraphic interpretation using shear and compressional seismic data: Geophysics, v. 49, p. 508-520.**

3. **McCormack, M.D., Justice, M.G., and Sharp, W.W., 1985, A stratigraphic interpretation of shear and compressional wave data for the Pennsylvanian Morrow Formation of southeastern New Mexico: p. 225-239 of AAPG Memoir 39, O.R. Berg and D.G. Woolverton, editors, Tulsa, Oklahoma, 276 pages.**

4. **Muller, M.C.. 1992, Using shear waves to predict lateral variability in vertical fracture intensity: The Leading Edge, v. 11, no. 2, p. 29-35.**

5. **Seismic MicroTechnology Inc., Houston, Texas.**

LIST OF ACRONYMS AND ABBREVIATIONS

C-wave: Converted wave. A reflected SV shear wavefield produced by P- to -SV mode conversions when a downgoing P-wave propagates through a series of interfaces.
9C: 9-component
P-wave: Compressional mode of a seismic wavefield.
S-wave: Any shear mode (C, SH or SV)
SH: Horizontal shear wave
SMT: Seismic Micro-Technology
V_p: P-wave velocity
Vs: S-wave velocity
VSP: Vertical seismic profile
SV: Vertical shear wave

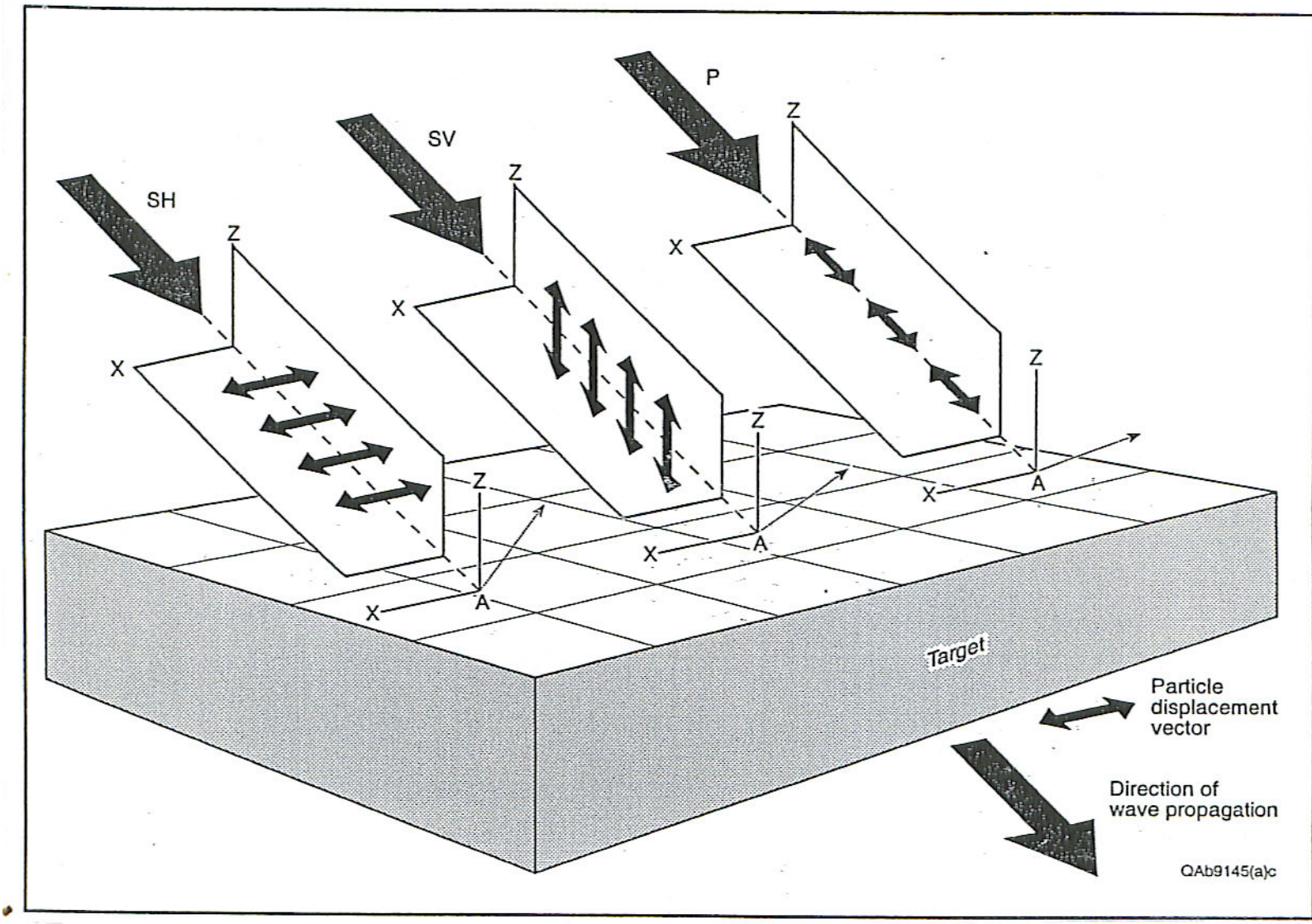

Figure 1. Propagation of the three fundamental modes, P, SH, and SV that comprise vector-wavefield seismic data.

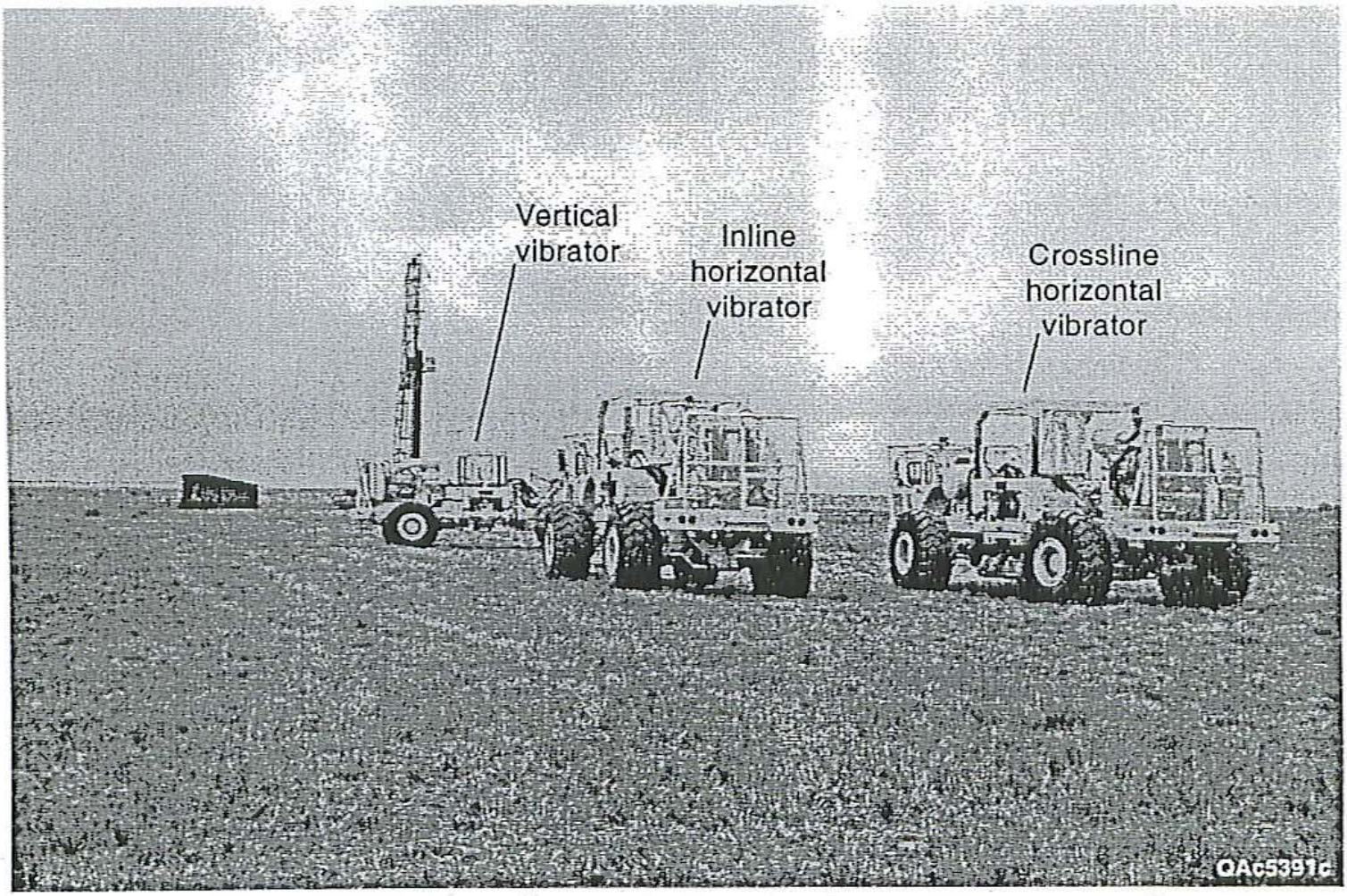

Figure 2. Orthogonal Vibrators used to generate 9C (9-component) VSP (Vertical Siesmic Profile).

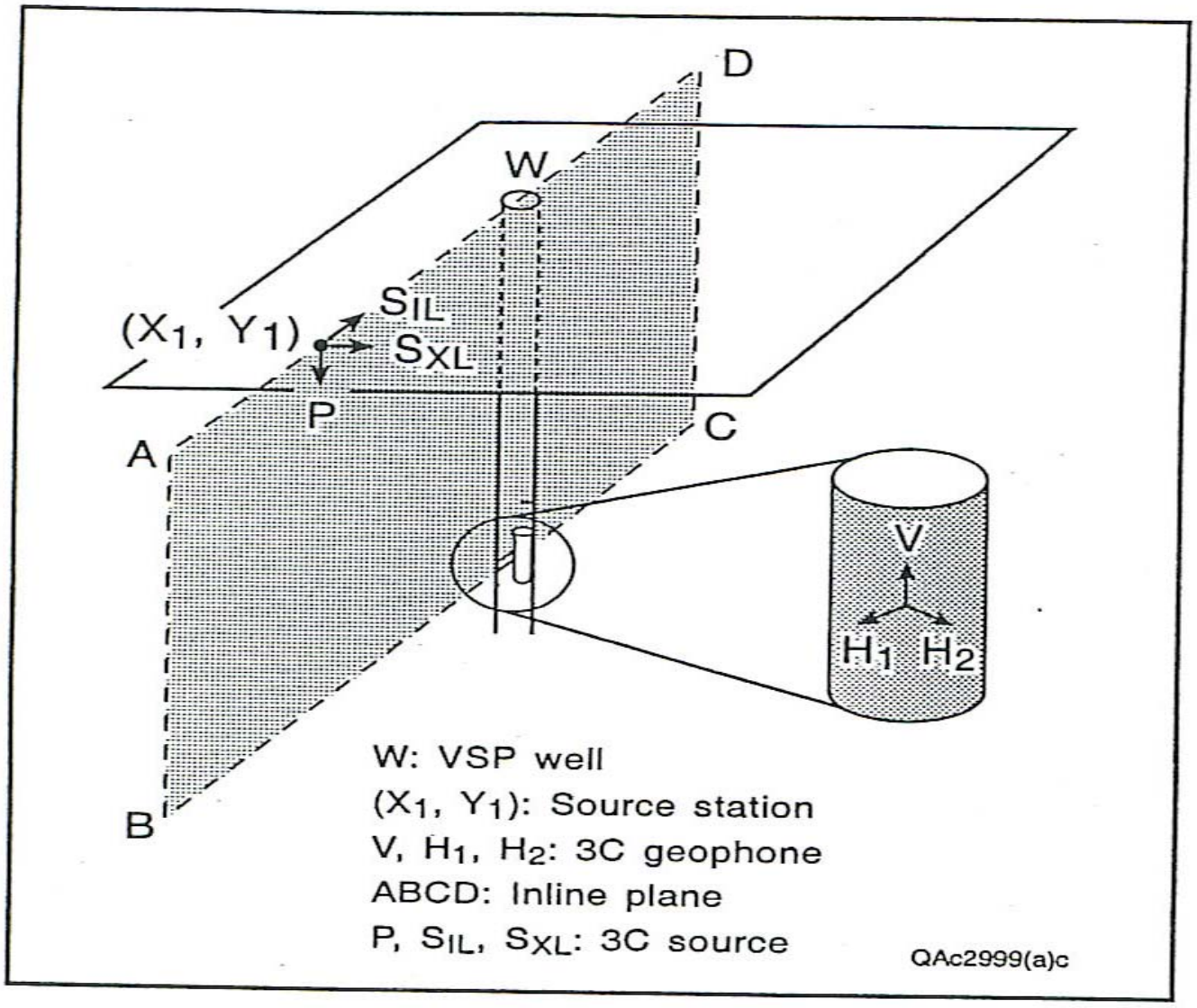

Figure 3. Fundamental geometry and key elements needed for 9C VSP data acquisiti

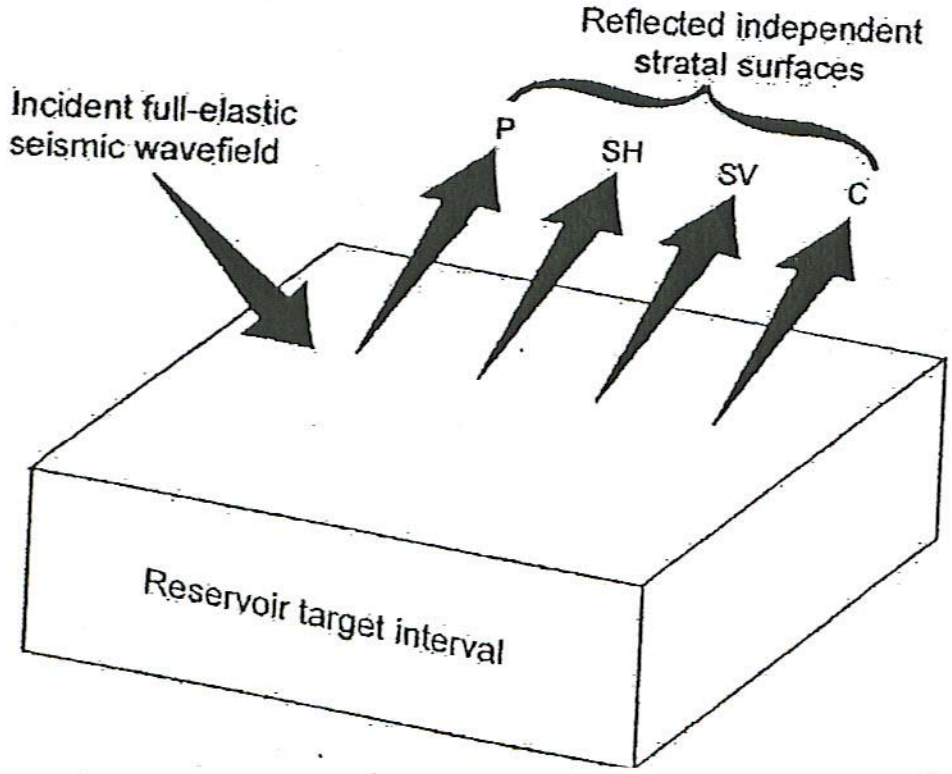

Figure 4. Comparison of conventional seismic stratigraphy and elastic-wavefield seismic stratigraphy. Conventional seismic stratigraphy utilizes only reflected P-wave modes. Elastic-wavefield seismic stratigraphy utilizes all elastic modes P, SH, SV, and C.

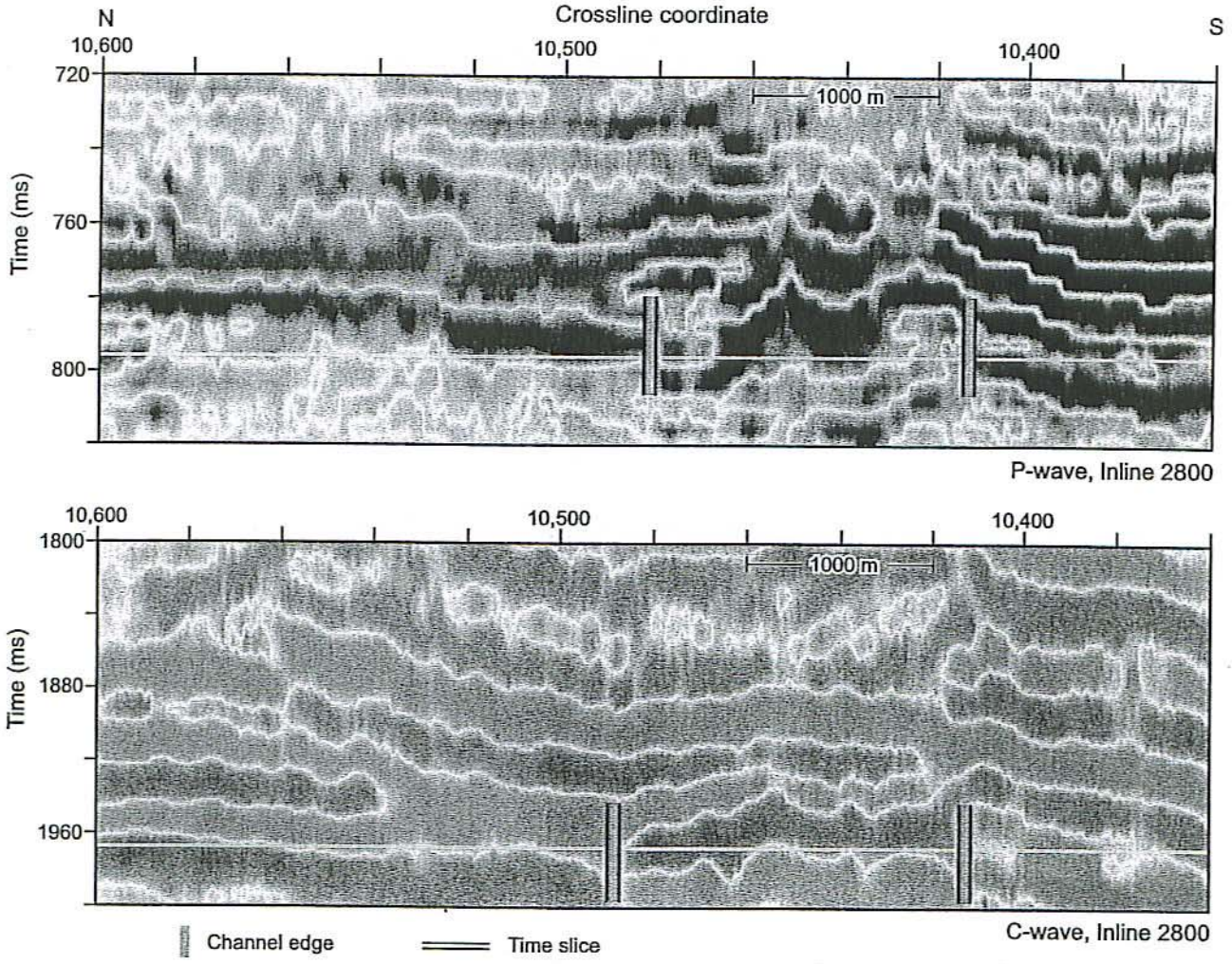

Figure 5. Inline profile 2800 across image target

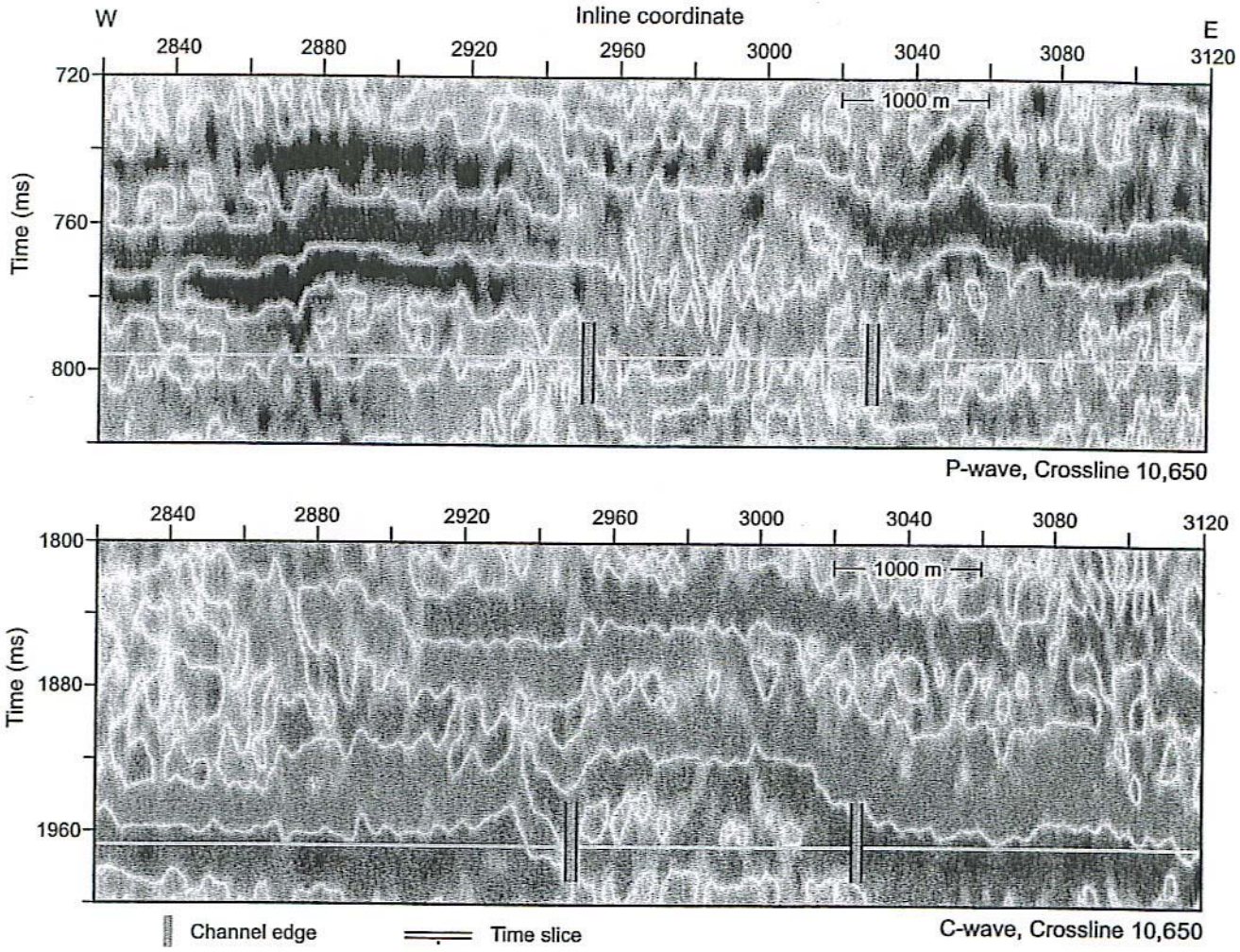

Figure 6. Crossline profile 10,650 across image target

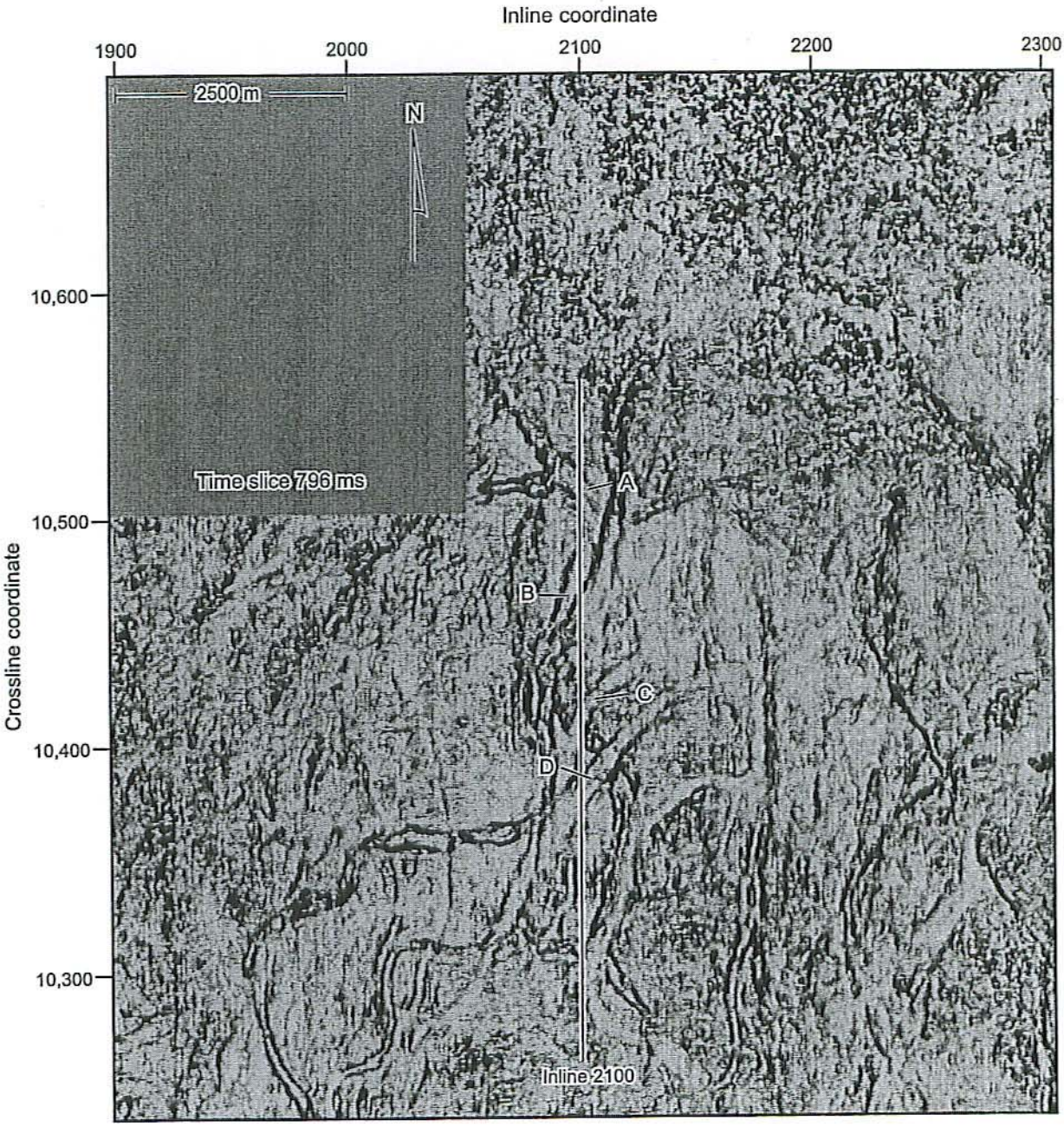

Figure 7. P-wave image search target

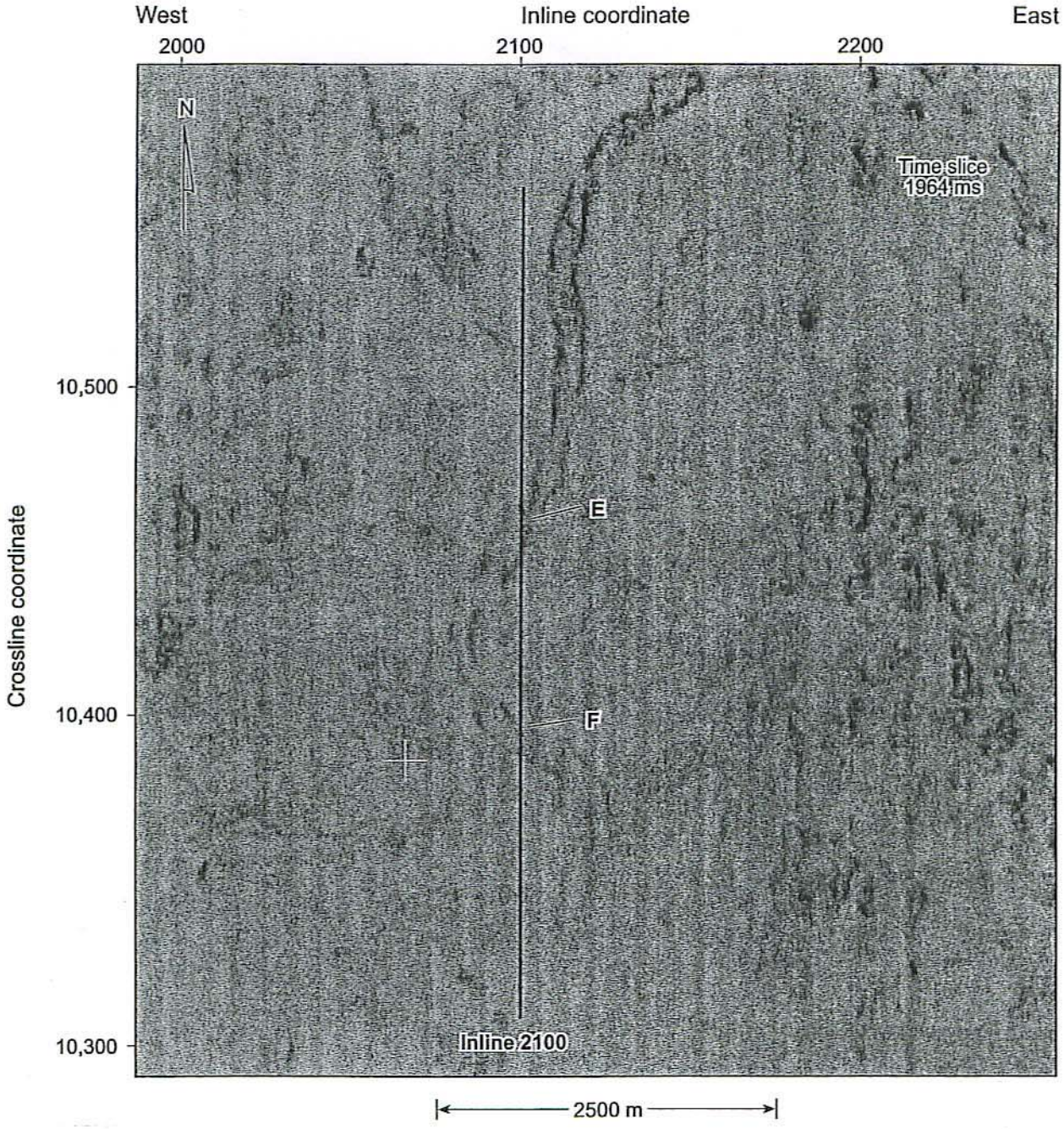

Figure 8. Depth-equivalent C-wave target

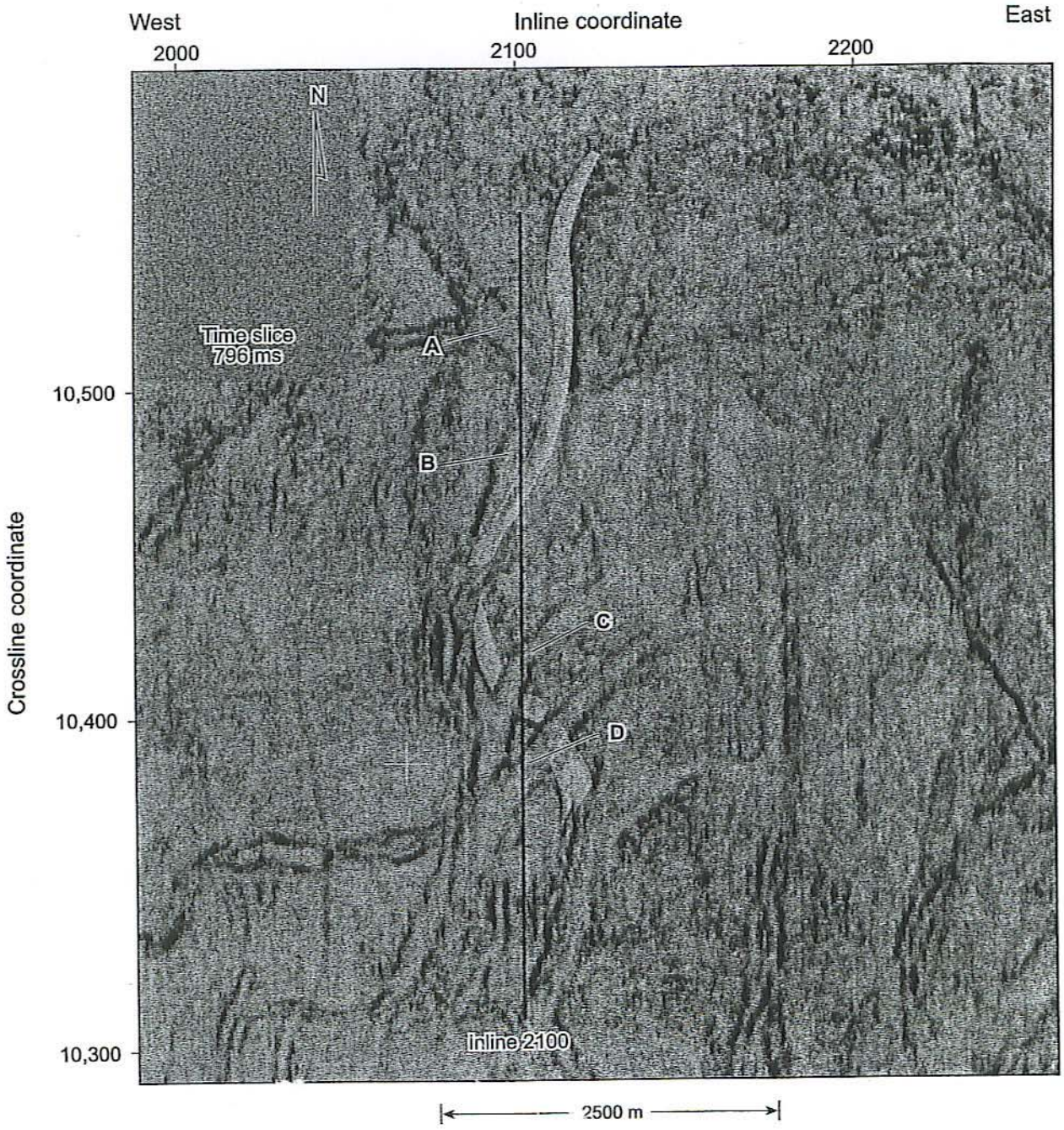

Figure 9. Comparison of P-wave and C-wave image targets.

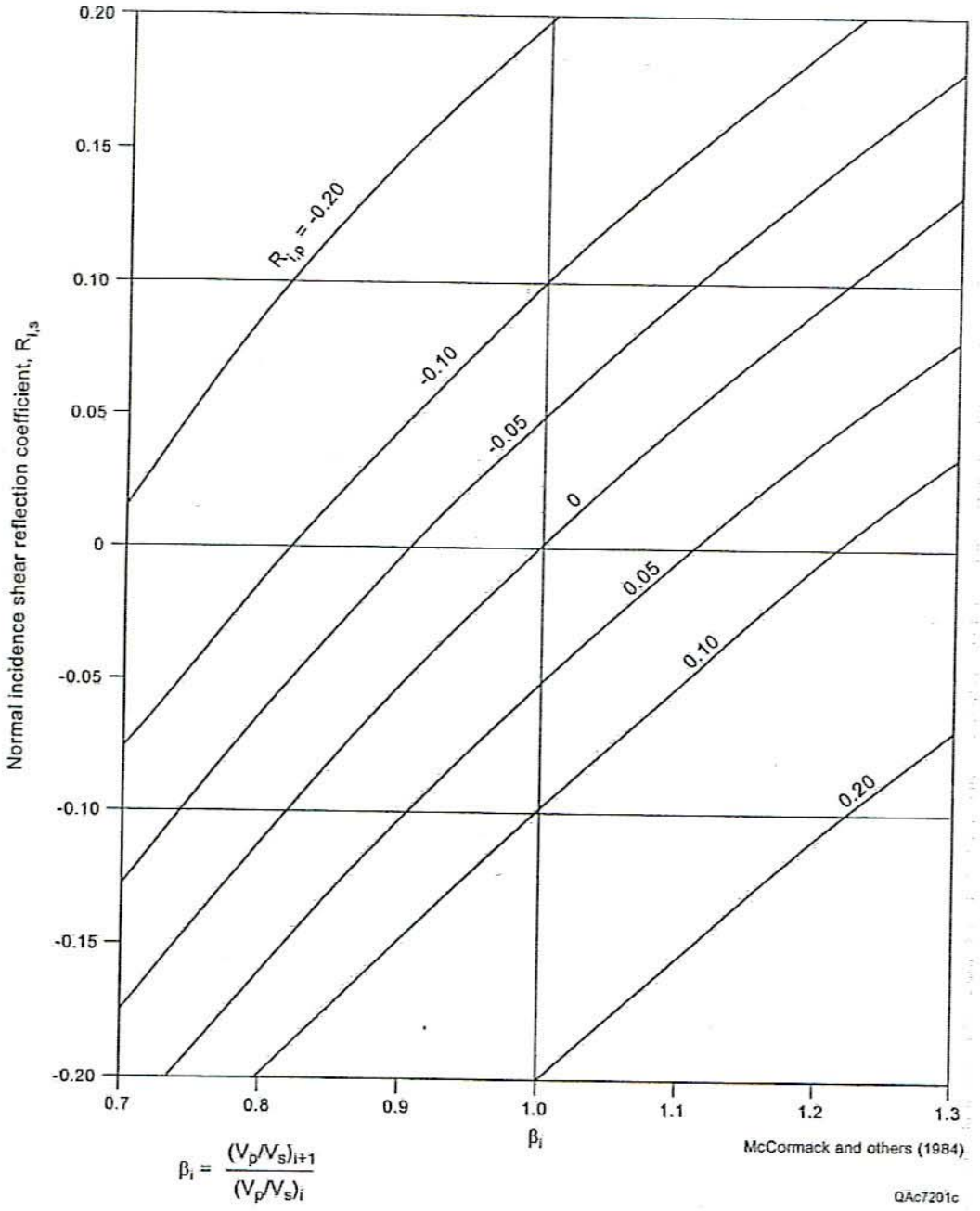

Figure 10.Contrast between P reflectivity $R_{i,p}$ and S reflectivity $R_{i,s}$ for vertical incidence on a stratal surface.